Journal of Hydroscience and Hydraulic Engineering
Vol. 19, No.2 November, 2001, 31-46

A NUMERICAL APPROACH TO SIMULATE HEAT AND MASS BUDGETS IN THE TOP SOIL AND LOWER ATMOSPHERE FOR DIFFERENT LAND-USE CONDITIONS

By

KUNIAKI SATO
Geosphere Research Institute, Saitama University, 255 Shimo-okubo, Saitama-shi, 338-8570, Japan

AKIRA WADA
Nihon University, College of Industrial Technology, 1-2-1, Izumi, Narashino, Chiba, Japan

TAKASHI SASAKI
Ark Information System, Gobancho, 4-2, Chiyoda-ku, Tokyo, Japan

and

RABINDRA RAJ GIRI
Geosphere Research Institute, Saitama University, 255 Shimo-okubo, Saitama, Japan

SYNOPSIS

The objective of this study is to predict quantitatively the water and heat budgets in soil and lower atmosphere for some typical surface elements using SALSA (Soil-Atmosphere Linking Simulation Algorithm) model. H. F. M. ten Berge first developed and used this model for bare soil case. The soil-atmosphere system is viewed as a one-dimensional system, and is subdivided into two semi-infinite domains by the soil surface. The transport processes for momentum, heat and mass in the atmospheric boundary layer and soil are described by means of well-established equations. The processes in the atmosphere and soil are linked to each other through the equations of heat and mass conservation. The moisture in the soil is treated as a two-phase mixture of liquid water and vapor. The simulated results are supported by the data recorded in a meteorological station from a newly developed residential area of Hanno district, Saitama Prefecture.

SALSA has so far been used only under simple surface conditions such as bare land. In this research, however, attempts have been made to apply it in surface conditions other than bare land. The typical surface elements used in this simulation are divided into four categories. They are bare land, soddy land, forest and porous paved surface. The simulation results provide heat and moisture balance scenarios for different urban elements. Based on the results, it will not be an exaggeration to conclude that the model can be applied at the city planning stage to predict quantitatively the influence of development on the environment.

INTRODUCTION

Evaporation is an important element for heat and moisture balance in the lower atmosphere and the topsoil and their transfer from one to another. On the other hand, evaporation is dependent on various surface characteristics such as roughness and canopy cover and soil composition, their thermal and hydraulic properties and incoming radiation. An understanding of the interaction between the topsoil

and the lower atmosphere through these transport processes is very important in order to predict heat and mass balance in these two domains.

Urbanization and industrialization have changed the characteristics of naturally occurring soil surfaces resulting in the disturbance of existing heat and moisture balance in the system. Increasing urbanization has brought about the increase of impervious and semi-pervious surface area. This phenomenon has reduced infiltration rates and evapotranspiration resulting in floods, submergence and decrease in groundwater table. These phenomena gradually change the heat and moisture balance in the vicinity of ground surface. As a result, modern cities are faced with serious meteorological and environmental problems. The elevated temperature in such big cities is an example of such impacts. The influences of the changes in ground surface uses on local micrometeorology can not be ignored since they have significant social implications. Therefore, it is necessary to quantitatively analyze these phenomena to predict the changes in heat and moisture balance due to changes in land use.

The comprehensive studies on the transport of coupled heat and moisture in soil have been conducted since the late 1950s. Phillip and De Vries (1957) developed a theory of moisture movement in soils under temperature gradients. There have been modifications in the previously developed theories and new theories also have been proposed for the simultaneous transport of heat and moisture in soils later. De Varies (1958) modified Phillip and De Vries theory. Sophocleous (1979) carried out an analysis for heat and water flow through saturated-unsaturated soils. Sang-ok et al. (1987) investigated the heat and water flow through soils partially covered with Mulch. Milly (1982) also investigated the same things in hysteric and inhomogeneous soils. Milly (1996) analyzed the effects of thermal vapor diffusion on seasonal dynamics of water in unsaturated soils. There are numerous other literatures available on heat and moisture transport in saturated-unsaturated soils. However, few studies have dealt with the interaction of lower atmosphere and soil surface for the transport of coupled heat and moisture in soils. J. Siebert et al. (1992) introduced a one-dimensional model for the simulation of transport processes at surfaces and in the atmosphere due to their interaction between different soils and vegetation. Brukaer et al. (1995) and Entekhabi et al. (1995) used an analytic approach to investigate the effects of soil-atmosphere interaction on different soil and atmospheric variables.

H.F.M ten Berge (1990) developed Soil-Atmosphere Linking Simulation Algorithm (SALSA) for the simulation of coupled heat and moisture transfer in soil and atmosphere due to the interaction between them. This simulation model has been used in bare soil cases and validated successfully. Because of its reliability in predicting soil and atmospheric variables for bare soil case, it has been chosen as a competitive model in this study to be used in other surface conditions. The soil-atmosphere system is viewed as a one-dimensional system, and is subdivided into two semi-infinite sections by the soil surface. The transport processes for momentum, heat and mass in the atmospheric boundary layer and soil are described by well-established transport equations. The processes in the atmosphere and soil are correlated to each other through the equations of heat and mass conservation.

The objective of this research is to predict quantitatively the heat and moisture budgets in soil and atmosphere due to the changes in land use. SALSA has so far been used under simple surface conditions such as bare land. In this work, attempts are made to use it for surface conditions other than bare soil. The typical surface elements in this study have been divided into four categories and they are bare soil, soddy land, forest and porous pavement. Different canopy resistance values, surface roughness heights, soil compositions and thermal and hydraulic soil properties characterize these surface elements. The soil thermal properties include soil emissivity, thermal heat conductivity; and soil hydraulic properties include porosity, hydraulic conductivity, residual water content, van Genuchten parameters and so on. Soil is considered to be composed of mainly five constituents and they are clay, organic matter, quartz, air and water. The soils under the four surface conditions consist of different soil compositions. The porous pavement is characterized by high value of quartz content and lower porosity in the simulation. Solar radiation and air temperature at screen height are used as

input variables in the simulation. These data are obtained from a meteorological station set in the Big Hill site of Hanno City, Saitama Prefecture.

COMPUTATION METHODOLOGY

The computational domains are mainly divided into three categories: they are surface, atmosphere and soil. The surface domain plays vital importance in the physical processes that occur in the other two. The atmospheric and soil domains are divided into eleven and twenty-five uneven horizontal compartments respectively. The compartments close to the surface have smaller thickness. The compartment thickness increases away from the surface. For simplicity, the domains in questions are assumed to be horizontally homogeneous. The computation starts with the imposition of initial and boundary conditions. The saturation water content for the top few centimeters of soil depth characterizes the rainfall condition. Then, surface energy balance is carried out for the given thermal and meteorological input data. The calculated surface temperature is the governing condition at the interface between the two remaining domains. This is followed by the computations of variable values in the atmosphere and soil respectively (Figure 1).

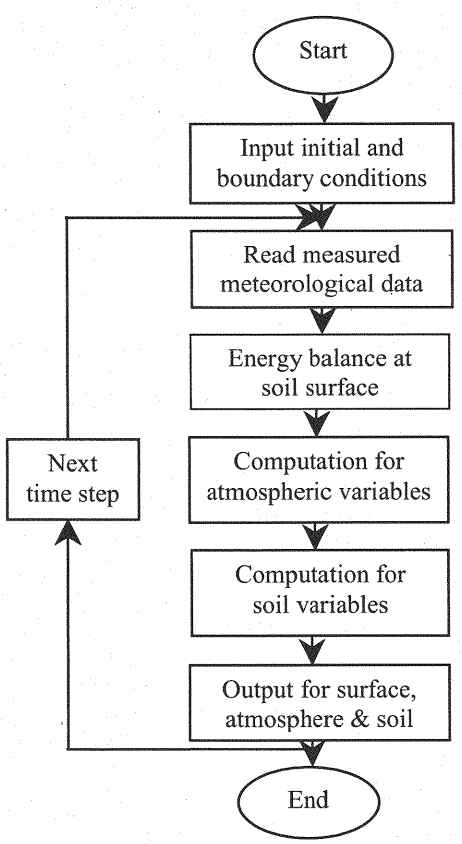

Figure 1. Computational flow diagram

ATMOSPHERE MODELING

The equations for momentum, heat and moisture transfer in vertical direction in the atmospheric domain are simplified into the following forms (ten Berge, 1990):

$$\frac{\partial u}{\partial t} = f\left(v - v_g\right) - \frac{\partial}{\partial z}\frac{\tau_x}{\rho} \; ; \; \frac{\partial v}{\partial t} = -f\left(u - u_g\right) - \frac{\partial}{\partial z}\frac{\tau_y}{\rho} \tag{1}$$

$$\frac{\partial \theta}{\partial t} = -\frac{\partial}{\partial z}\left(\frac{H}{\rho C_p}\right) \; ; \; \frac{\partial q}{\partial t} = \frac{\partial}{\partial z}\left(\frac{E}{\rho}\right) \tag{2}$$

where u and v = the two orthogonal components of horizontal wind velocity, u_g and v_g = the corresponding geostrophic velocities, f = the Coriolis parameter, ρ = the air density, q = the moisture mixing ratio (kg of water/ kg dry air), H = the sensible heat flux, E = the vapor flux (kg/m^2-sec.), θ = the potential temperature, C_p = the specific heat of air at constant pressure and τ = the shear stress.

The momentum, sensible heat and vapor flux transport can be written using eddy diffusivities $K_{M,H,V}$ as follows:

$$\tau_x = -\rho K_M \frac{\partial u}{\partial z} \; ; \; \tau_y = -\rho K_M \frac{\partial v}{\partial z} \tag{3}$$

$$H = -\rho C_p K_H \frac{\partial \theta}{\partial z} \; ; \; E = -\rho K_v \frac{\partial q}{\partial z} \tag{4}$$

Where the subscripts M, H and V denote momentum, sensible heat and vapor respectively. The eddy diffusivity is given by the following equation:

$$K_{H,M,V} = l_{M,H,V}\left(Ce\right)^{0.5} \tag{5}$$

The length scales $l_{M,H,V}$ are computed from the similarity functions $\phi_{M,H,V}$ as follows:

$$l_{M,H,V}^{-1} = \frac{\phi_{M,H,V}(\zeta)}{\kappa z} + \frac{f}{\alpha u_g} \tag{6}$$

In equation (6), ζ = stability parameter given by z/L, L = Monin-Obukhov length scale, k = the Von Karman constant and α and C are empirical constants equal to 4.0×10^{-4} and 0.2 respectively. The system is closed by the equation for turbulent kinetic energy e (TKE) given by the following equation (Tennekes & Lumley, 1972):

$$\frac{\partial e}{\partial t} = \frac{\tau_x}{\rho}\frac{\partial u}{\partial z} + \frac{\tau_y}{\rho}\frac{\partial v}{\partial z} + \frac{g}{T}\frac{H}{\rho C_p} + \frac{\partial}{\partial z}K_M\frac{\partial e}{\partial z} - \frac{(ce)^{3/2}}{l_M} \tag{7}$$

Where, T is air temperature (K).

The equations for momentum, sensible heat and vapor transport in the vicinity of the ground surface are given as follows:

$$\tau_x = \rho \frac{u(Z_m) - u(Z_0)}{r_{aM}} \; ; \; \tau_y = \rho \frac{v(Z_m) - v(Z_0)}{r_{aM}} \tag{8}$$

$$H = \rho C_p \frac{T(Z_m) - T(Z_0)}{r_{aH}} \; ; \; E = \rho \frac{q(Z_m) - q(Z_0)}{(r_{aV} + r_s)} \tag{9}$$

Where, u and v = horizontal wind velocities along x and y-axes respectively, Z_0 = roughness height (m), Z_m = height at which the state variables are measured or calculated (m), T = air temperature, q = moisture mixing ratio, r_a = aerodynamic resistance (s/m) and r_s = vegetation resistance (s/m). The subscripts M, H and V denote momentum, sensible heat and vapor respectively.

HEAT AND MOISTURE TRANSPORT IN SOIL

The problem of unsaturated flow induced by evaporation and integrated coupling of heat and mass has been discussed in many studies (Phillip & De Vries, Milly, Tzimopoulos, Fukuhara et al.). The one-dimensional heat transport equation in soil domain used in this simulation is expressed by the following equation:

$$C_s \frac{\partial T_s}{\partial t} = \frac{\partial}{\partial z}\left(\lambda \frac{\partial T_s}{\partial z} + J_v H_v \right) \tag{10}$$

Where, T_s = soil temperature, J_v = water vapor flux (kg/m^2-sec.), H_v = latent heat of vaporization for water (J/kg), C_s = volumetric heat capacity for soil (J/m^3-K) and λ = thermal conductivity (W/m-K). The volumetric heat capacity and thermal conductivity are calculated using De Vries formulae (De Vries, 1963 and 1975) as follows:

$$C_s = \sum_1^n f_i C_i \; ; \; \lambda = \frac{\sum_1^n k_{ij} f_i \lambda_i}{\sum_1^n k_{ij} f_i} \tag{11}$$

Where f_i, = fraction of the ith soil constituent, C_i and λ_i = volumetric heat capacity and thermal conductivity for the ith constituent in soil respectively and k_i = weighting factor for specific thermal conductivity for ith soil constituent relative to that of water. The soil particles are regarded as spheroids. The weighting factors k_{ij} are given by the following equation (De Vries, 1975):

$$k_{ij} = \frac{2}{3}\left(1 + \left(\frac{\lambda_i}{\lambda_j} - 1 \right) g_i \right)^{-1} + \frac{1}{3}\left(1 + \left(\frac{\lambda_i}{\lambda_j} - 1 \right)(1 - 2g_i) \right)^{-1} \tag{12}$$

Where, j refers to water, and g_i = shape factor for soil particles of ith constituent. In this simulation, the shape factor values used are 0.20, 0.01, 0.50, 0.14 and 0.14 for air, clay, organic matter, quartz and water respectively (ten Berge, 1990).

The water in the soil is treated as two-phase mixture of liquid and vapor. The one-dimensional transport equation for liquid phase is expressed in the following form:

$$\rho_l \frac{\partial \theta_w}{\partial t} = \frac{\partial}{\partial z}\left[K(\theta_w, T_s) \frac{\partial p(\theta_w, T_s)}{\partial z} \right] - \rho_l g \frac{\partial}{\partial z} K(\theta_w, T_s) \tag{13}$$

Where, p = pressure potential (Pa), K = Hydraulic conductivity (kg/m-Pa-sec.), ρ_l = liquid water density (kg/m^3), g = acceleration due to gravity (m/sec.^{2}) and θ_w = volumetric liquid water content.

The equivalent transport equation for the vapor phase is expressed by using the following form:

$$\rho_l \frac{\partial \theta_v}{\partial t} = \frac{\partial}{\partial z}\left[D_e(\theta_v, T_s) \frac{\partial \rho_v(\theta_v, T_s)}{\partial z} \right] \tag{14}$$

Where, ρ_v = water vapor density (kg/m^3), θ_v = volumetric water vapor content and D_e = effective vapor diffusion coefficient (m^2/sec.).

Auxiliary Equations

Equation (10), (13) and (14) are the main transport equations for heat and moisture in the soil domain. Some of the variables in these equations need to be specified in terms of other soil parameters to have their solution in numerical simulation. The pressure potential function is expressed by the following equation (Van Genuchten, 1980):

$$p = -\frac{1}{\alpha}\left(Se^{-1/m} - 1\right)^{1/n} \tag{15}$$

Where α = Van Guchten parameter (Pa^{-1}), m & n = Van Guchten parameters and Se = relative moisture content, which is expressed by the following equation:

$$Se = \frac{\theta_w - \theta_r}{\theta_s - \theta_r} \quad (0 \le \mathrm{Se} \le 1) \tag{16}$$

In equation (16), θ_s = saturated volumetric water content and θ_r = residual volumetric water content. The soil hydraulic conductivity is expressed by the following equation (Mualem, 1976):

$$K = K_s Se^{1/2}\left\{1 - \left(1 - Se^{1/m}\right)^m\right\}^2 \tag{17}$$

In the above equation, K_s = saturated hydraulic conductivity and m = 1 – 1/n ($0 \le m \le 1$, $n \ge 1$), which depends on the inclination of moisture characteristic curve. The density gradient of water vapor is expressed by the following equation (Phillip and De Vries, 1957):

$$\frac{\partial \rho_v}{\partial z} = \left(\frac{\partial \rho_v}{\partial T}\right)_\theta \frac{\partial T}{\partial z} + \left(\frac{\partial \rho_v}{\partial \theta}\right)_T \frac{\partial \theta}{\partial z} \tag{18}$$

The first and the second terms on the RHS of equation (21) are called "thermal" and "isothermal" terms respectively. The water vapor flux due to diffusion (J_v) is expressed by the following equation:

$$J_v = -\beta D_a(T) \frac{\partial \rho_v(\theta_v, T)}{\partial z} \tag{19}$$

Where β = vapor diffusion enhancement factor (Cary, 1963) and D_a = diffusivity of vapor in free air (m^2/sec.).

FIELD DATA AND SIMULATOIN

Field Observation Site

Meteorological and thermal data obtained from the meteorological station that is established in the new Hanno residential development area is used as input in this simulation study. The Hanno measurement site lies on a hillside about 45 km to the south of inner Tokyo in Saitama Prefecture. The development zone is a part of a planned community that is known as "Hanno Big Hills". The geology of the site consists of an alluvium above a basement in the Mesozoic and Paleozoic era and the upper layer is covered with talus, river deposits and unconsolidated gravel. The original topography of the project site is mountainous with steep slopes in valleys at 30 to 40 degrees. The soil permeability is small since the formation of mountain is covered by soft cemented gravel. A large-scale land development work is underway in the area. According to the plan, 137.7 hectare of natural forest will be converted to a new city. Out of the total area, 30% will be used for residential complexes, 26% for public facilities and the rest for transportation and green area. It is vitally important to study and predict the local hydrological and thermal characteristics due to the land development before its implementation. In this way, necessary countermeasures can be taken to restore the local hydrological and thermal environment in the area.

Observation System

Figure 2 shows a schematic diagram of the measurement system established in the Big Hill Site. The meteorological variables such as air temperatures at two heights (0.5 and 1.0 m), humidity (wet and dry-bulb), solar radiation, ground heat flux, albedo, precipitation, atmospheric pressure, wind speed and its direction are recorded every minute by means of this system. Apart from this, soil samples are taken from different depths to determine some soil hydraulic properties in the laboratory. Temperature sensors (thermocouples) are embedded at different soil depths to record soil temperature, which is used to compare with the simulated temperatures.

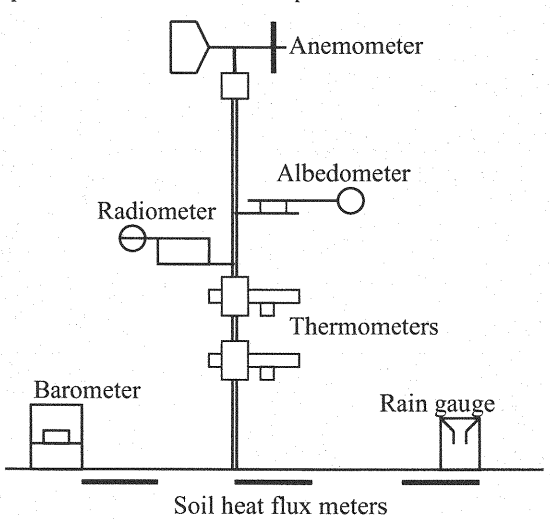

Fig. 2 Measurement system

Parameterization of Land-Use Elements

Figure 3 shows schematically the conceptual models for the four selected land-use elements in the simulation. Soil composition, surface roughness parameters and soil hydraulic and thermal properties

characterize these elements. Surface roughness parameters include soil surface roughness height and vegetation resistance. Soil hydraulic and thermal properties include hydraulic conductivity, Van Guchten parameters, thermal conductivity, soil emissivity and soil heat capacity. The numerical values for these parameters are adopted from available literature (T. R. Oke, 1978; J. R. Garrat, 1992 and so on). Bare land means the land without vegetation and the minimum value of surface roughness height has been used in this case. Soddy land means grassland with vegetation height of about 10 cm from the surface. Forest includes a land element having dense trees with the height of about 10-meter. In this case, the roughness height and vegetation resistance values are large. The porous pavement is concrete pavement designed for the interception and percolation of precipitation to prevent excess overland flow. High quartz content and relatively lower porosity values characterize it. The typical parameter values for the selected land-use elements in this simulation are shown in table 1.

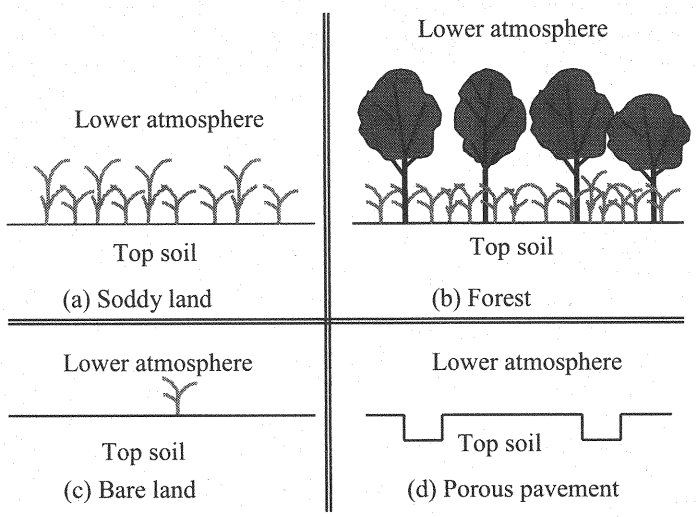

Fig 3 Conceptual models of land-use elements

Table 1 Principal parameters used in the simulation

Parameters	Bare land	Soddy land	Forest	Porous pavement
Surface roughness height (m)	0.001	0.01	0.80	0.001
Vegetation resistance (s/m)	0.0	10.0	100.0	0.0
Soil porosity (m^3/m^3)	0.40	0.45	0.50	0.25
Saturated soil hydraulic conductivity (cm/s)	1.4×10^{-6}	5.0×10^{-6}	1.0×10^{-5}	1.0×10^{-8}

Initial and Boundary Conditions in Simulation

The atmospheric domain extends up to 3069-meter height from the ground surface in the simulation. It is divided into eleven uneven horizontal compartments, which are assumed to be horizontally homogeneous. The boundary conditions at this upper boundary level are set as: $u = u_g$, $v = v_g \equiv 0$, $\tau_x = \tau_y = 0$, $H = 0$, $E = 0$ and $\partial e/\partial z = 0$. The groundwater table is fixed at a depth of 1.60

meter from the surface. The soil domain is divided into twenty-five uneven horizontal meshes. The conduction heat flux and liquid water flux are equated to zero as the lower boundary conditions for heat and moisture at this depth. At the surface, it is assumed that there is no storage of heat and mass. Equations (8), and (9) govern for the surface layer boundary conditions, where the value of turbulent kinetic energy flux is taken to be zero. The initial and boundary conditions for simulation are shown in figure 4.

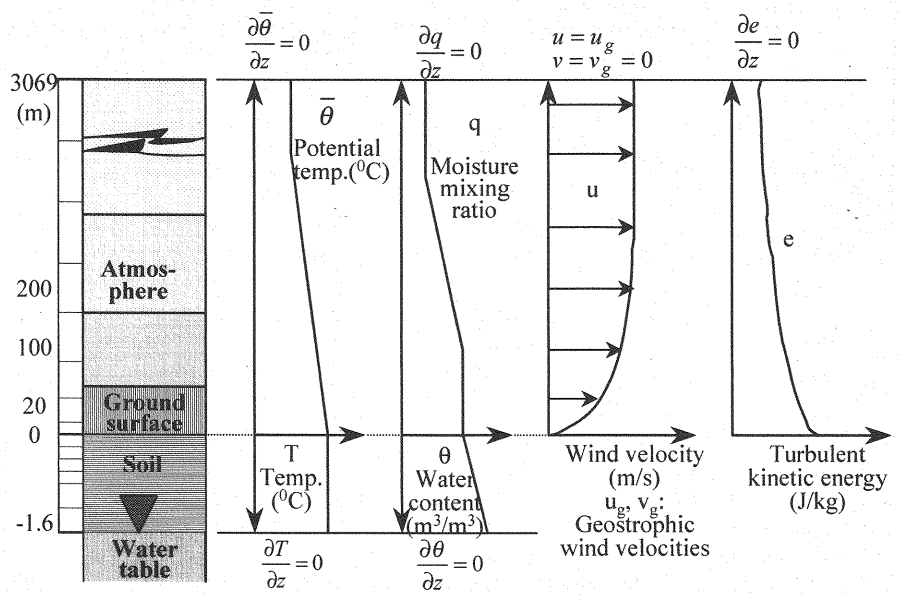

Fig. 4 Initial and boundary conditions in SALSA

The conditions with and without rainfall are characterized by the initial soil water contents. For no rainfall condition, the topmost soil compartment has the smallest initial soil water content. This value increases downward and becomes saturated at the bottom boundary where the water table is fixed. For rainfall conditions, the top five-centimeter of the soil depth is saturated with as initial soil water content. Below this depth, the values are the same as under the conditions of no rainfall.

RESULTS AND DISCUSSIONS

The simulation was carried out with the meteorological data from August 4, 1998 to August 7, 1998 obtained from the Hanno Site. The validity of this simulation model for bare agricultural land was checked by H.F.M. ten Berge (ten Berge, 1990). Its validity and accuracy for bare soil in Hanno Residential Development area was checked by Pham et al. (1999). In this study, attempts were made to extend its application for other urban elements. Only the significant findings of the simulation results are discussed in the next paragraphs.

Figure 5 shows the variation of temperature and water content at different depths for bare soil during the simulation period. The variation is maximum for the surface layer and this effect decreases downwards. The impact of soil-atmosphere interaction in soil heat and moisture fluctuations is observed to be effective up to depths of 15 to 20-cm from the surface. As simulation progresses, the subsoil temperatures tend to increase, which is due to heat conduction to subsoil during daytime strong radiation. On the other hand, the soil water content tends to decrease. An increase of evaporation rate during daytime was the cause of such a decrease. Field measurement of these parameters was carried out on August 6, 1998 to crosscheck the simulated results for bare soil case. Even though there are

few measured data, they agree with the simulated results. Since the accuracy of the model for bare soil case is already checked, this cross-check by means of few available measured data is sufficient for the time being.

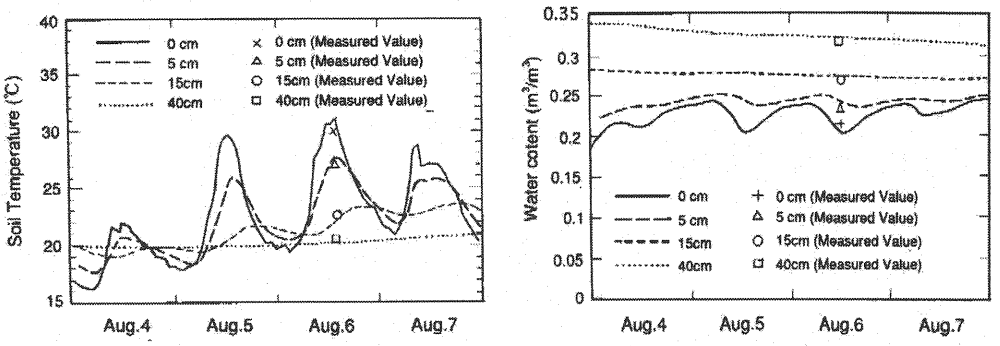

Fig. 5 Comparison of simulation results with measurements

Comparison between Bare land and Forest

Figure 6 and 7 show energy fluxes during the simulation period, soil temperature, and water content profiles along the soil depth at three different times in a day for bare land and forest. The net radiation flux for the whole simulation period is smaller for the forest-covered surface than for bare land. It is evident that canopy cover has a radiation shielding effect resulting in lower value of net radiation flux. The canopy cover also affects the latent heat flux. At noon when the incoming radiation is strong, the latent heat flux is the maximum for bare land, and decreases to its minimum values at nighttime. This heat flux for bare land is mainly due to evaporation. However in the case of forest element, this peak value at noon decreases, and the minimum values at nighttime increase. This is due to the shielding and evapotranspiration effects of the canopy cover. During the daytime, the radiation shielding effect of the canopy cover decreases net radiation resulting in a decrease in evaporation and hence the latent heat flux. At nighttime, the net evaporation increased due to transpiration even though the evaporation from the soil surface is very small. The sensible and ground heat fluxes seem to be affected only slightly in these cases. However, the canopy covered surfaces showed decreasing tendency.

The temperature variations at and near the surface in the soil domain are more in cases of bare land (Fig. 7 and 8). The shielding effect of canopy cover reduces the net radiation exposure to the soil surface. At the same time, canopy cover decreases wind speed near the surface resulting in low values of latent heat flux. In the morning, the temperature near the surface is observed below the initial value used for the simulation (20^0 C) in bare land case, and at noon it reaches more than $30\ ^0$ C. In case of the forest, this variation is relatively smaller.

The contrast in soil water distributions is clear in these two cases, which can be seen from the figures. The amplitude of soil water fluctuation during the day at and near the soil surface in bare land is high, but it is negligible in forest element. The high values of net radiation flux and wind speed are the main reasons for these fluctuations. In case of forest covered land, evaporation from soil surface gets reduced due to shielding effect of canopy. Even though transpiration contributes to evaporation, the former is always dominated by the later. On the other hand, forest covered soil may contain higher fractions of humic substances resulting in relatively higher hydraulic conductivity values and faster capillary rises from groundwater table.

Figure 8 shows wind velocity profiles in atmospheric domain at three different times of a particular day for bare land and forest. At 1.50 meter height from ground surface, the horizontal component of

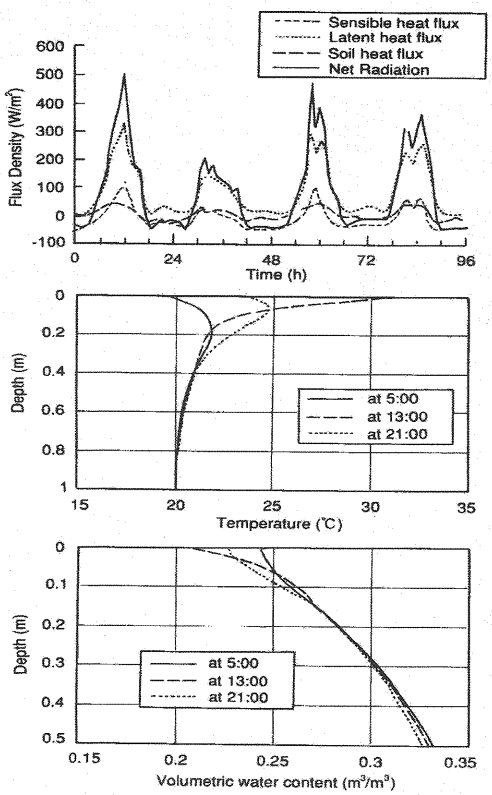

Fig. 6 Simulation results for bare land (based on the data of July 5~9, 1998)

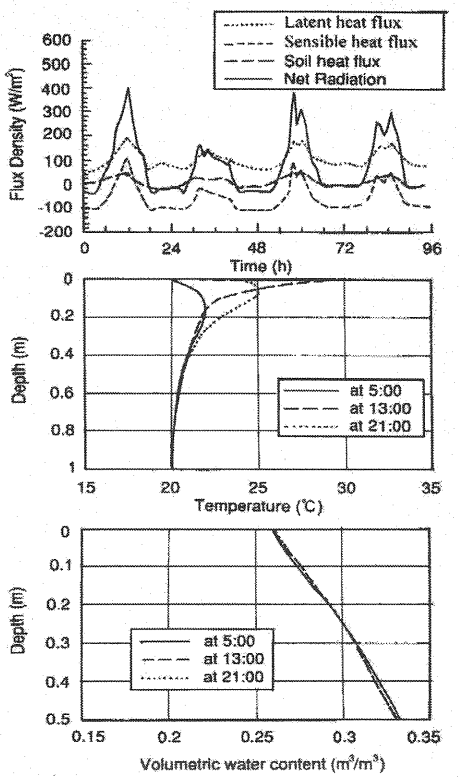

Fig. 7 Simulation results for forest (based on the data of July 5~9, 1998)

wind velocity for bare land case is about five times of the value for forest due to differences in surface roughness heights. As the surface roughness height increases, its effect on wind velocity reaches the upper part of the atmospheric domain, which is depicted in figure 8. The wind velocity has smaller values at the mid-day and increased in the evening and at night in that particular day of the simulation. The simulation results showed that the atmospheric conditions seem to be more stable in the daytime than in the evening and at night.

Figure 9 shows the liquid water content distribution along the soil depth at different times after the rainfall for bare land and forest. The fluctuation amplitude for this parameter at and near the surface is greater for bare land cases compared to conditions where there is no rainfall (Fig. 6). This amplitude is not negligible in forest case as it is in no rainfall condition. As time passes after rainfall, the water content values for bare land conditions decrease in general. For about 10 to 15-cm topsoil layer, it decreases rapidly within 24 hours. This value increases from about 15 to 40-cm depth from the top. But it seems to decreases slightly below this depth. This interesting behavior of soil water content distribution can be attributed to mainly the surface characteristics of bare land. Due to the absence of a canopy cover, the net radiation is strong and evaporation is greater at the surface. As for forest covered land, this distribution is different from bare land. It decreases for the top few centimeters of soil, and then increases for the remaining depth. The decrease near and at the surface is smaller than its values for bare land. Since canopy cover has a shielding effect for radiation and evaporation from surface, there is smaller water loss as evaporation. On the other hand, forest covered soils contain

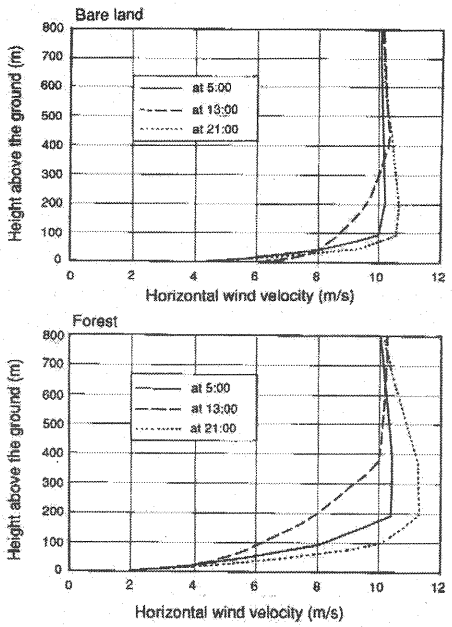

Fig. 8 Comparison of wind velocity distribution between bare land and forest (based on the data of July 5~9, 1998)

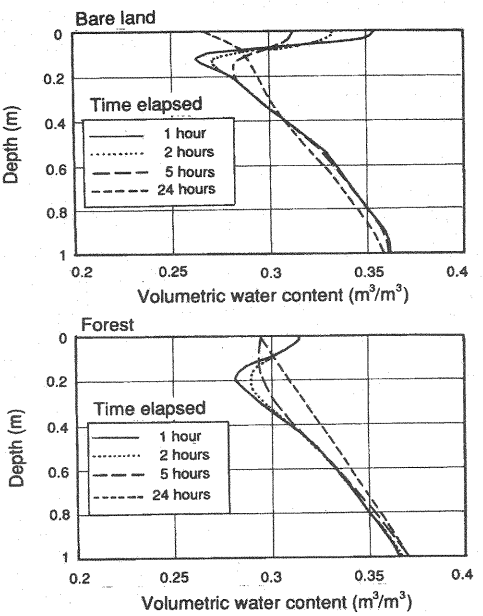

Fig. 9 Comparison of soil moisture changes due to rainfall infiltration between bare land and forest (based on the data of July 5~9, 1998)

relatively bigger fractions of humic substances, which increases hydraulic conductivity of the soil, the liquid water from rainfall easily percolates towards down.

Surface Temperature and Vapor Flux for Different Land-Use Conditions

Figure 10 shows a composite land-use model consisting of bare land, soddy land, forest, porous pavement and park. Parks can be considered as a combination of soddy land and forest. Since the surface temperature and vapor flux play important role in characterizing different urban elements, this section will focus on comparing these parameters in different land-use conditions.

Figure 10 shows surface temperature distributions in the composite land-use models at three different times of the day. The temperature distributions indicate that the minimum values reach before sunrise. The temperature values at 05:00 hrs are in the range of 17^0C and 20^0C in the entire model. However, the porous pavement and forest elements respectively exhibit the lowest and the highest surface temperatures at this time. The differences in surface temperature for the selected surface conditions become most noticeable at 13:00 hrs. The porous pavement surface reached about 40^0C, which is about 8^0C higher than in forest covered condition at this time. At 21:00 hrs, almost the same surface temperatures are observed for all the surface conditions.

In the above observations of surface temperature variations, the porous pavement element exhibited the most noticeable diurnal temperature change. The amplitude of this variation between 05:00 hrs and 13:00 hrs was about 25^0C. Another clear observation was the porous pavement, which exhibited both the highest and the lowest surface temperatures in diurnal fluctuations. On the other hand, the forest-covered surface exhibited the least variation in surface temperature, whose maximum amplitude was about 12^0C. Next to the porous pavement, the bare land exhibited a sharp surface temperature variation followed by soddy land. From our analysis of the simulation results, it can be quantitatively

concluded that forest-covered land and porous pavement respectively have the minimum and the maximum amplitudes for surface temperature variations during the day.

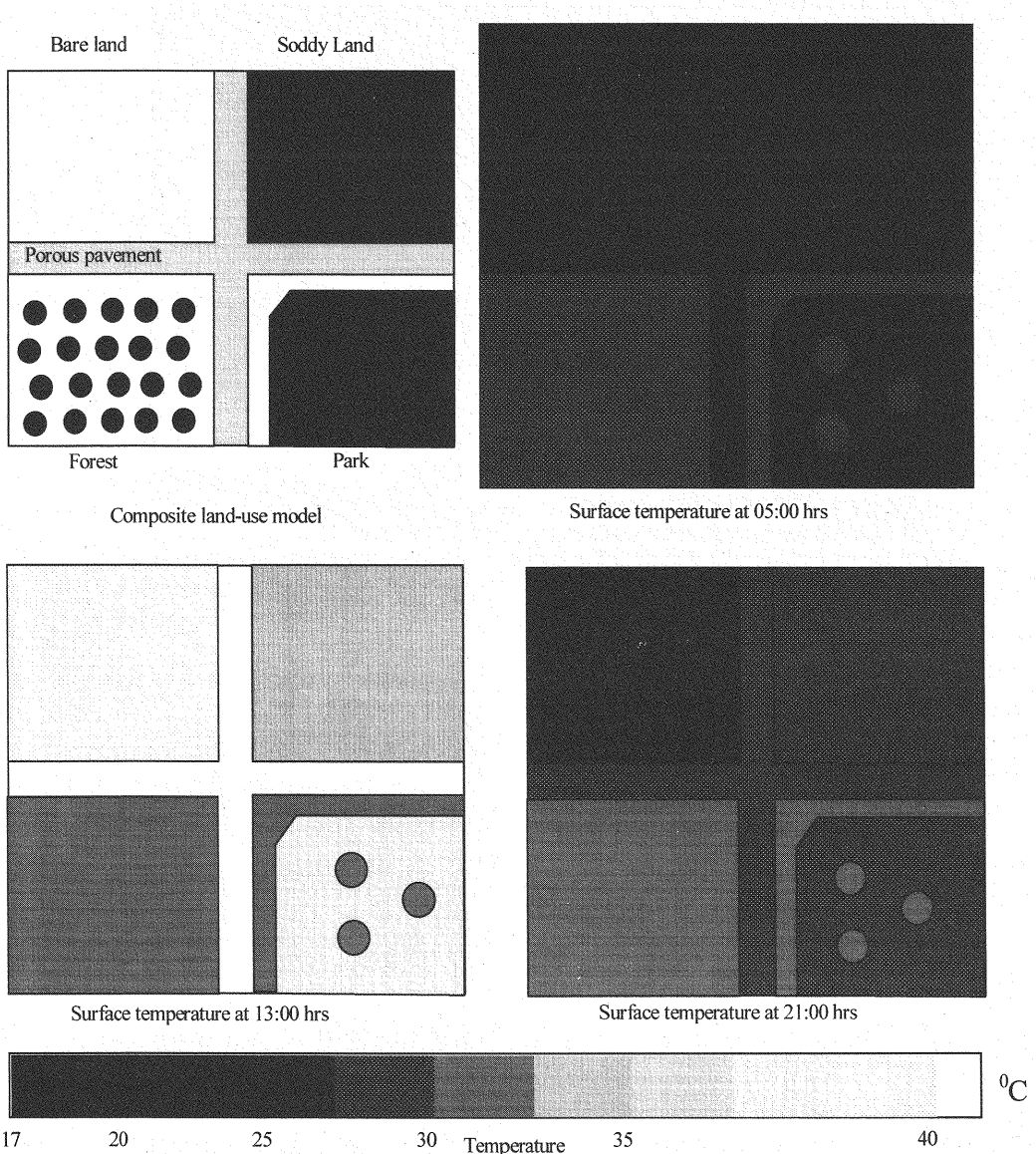

Fig. 10 Comparison of day and nighttime surface temperature distribution in the Composite land-use model (data July 5~9, 1998)

Figure 11 shows the water vapor flux density at the surface for the composite land-use model at 05:00 hrs and 13:00 hrs of the day. At 05:00 hrs, the forest element and the porous pavement respectively have the highest and the lowest values of water vapor flux density. However, at 13:00 hrs, bare land has the highest value. Then come soddy land, park, forest and porous pavement in the decreasing order. The maximum flux density value at 05:00 hrs is only about 36% of the minimum value at 13:00 hrs. At 13:00 hrs, the value for forest is only about 65% of the bare land. In case of soddy land, it is about 15% less than that of bare land. For porous pavement, the flux density has the

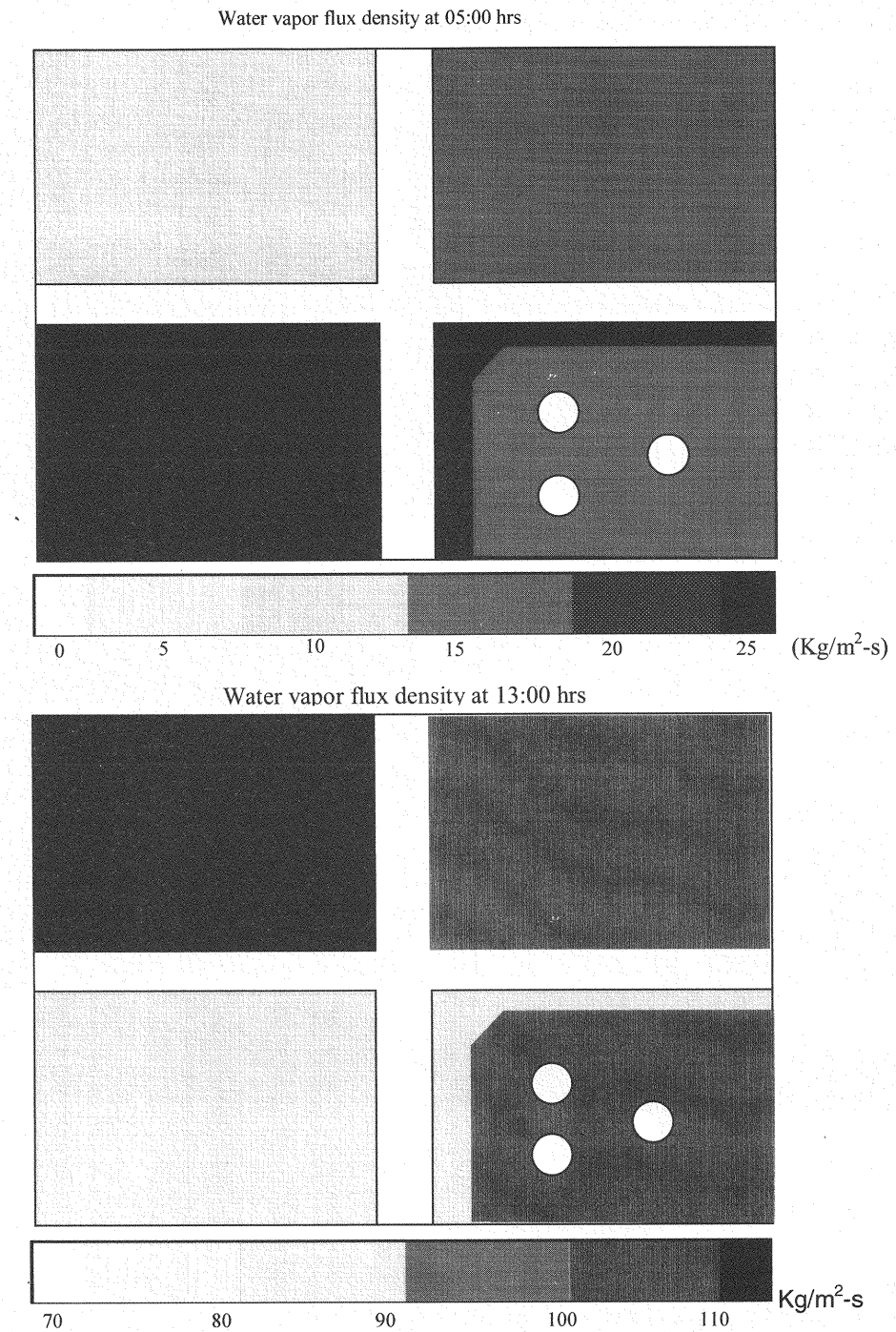

Fig. 11 Comparison of water vapor flux density in the composite land-use model (data July 5~9, 1998)

smallest value throughout the day. When the surface temperatures have their minimum values, forest element appears to have greater vapor flux density, which is probably due to evapotranspiration. At such times, bare land surface undergoes less evaporation compared with evapotranspiration in forest-covered land. When there is strong solar radiation, evaporation in bare land increases drastically. However, the shielding effect of the canopy cover prevents incoming radiation and evaporation, resulting in small vapor flux in forest-covered land.

CONCLUSIONS

Numerical simulations were carried out to predict heat and moisture budgets in the lower atmosphere and topsoil for four typical land-use elements. Soil-Atmosphere Linking Simulation Algorithm (SALSA) was one of the effective simulation models used in this study. The four typical land-use elements selected in this study are bare land, soddy land, forest and porous pavement. The concept of canopy resistance was introduced in the model to incorporate the effect of vegetation in heat and moisture budgets in the domains. Meteorological data obtained from the meteorological station of Hanno New Residential Development Area was used as input in the simulations. The following conclusions were drawn based on our analysis of simulation results.

(1) The amplitude of surface temperature fluctuation is the highest for porous pavement and the lowest for forest. Bare land and soddy land have the second and the third highest values respectively.
(2) During the daytime, bare land showed the fastest rate of evaporation. But, forest covered surface exhibited its maximum value at night, and porous pavement showed the lowest values in the day. In terms of soil water content, bare land and forest covered land respectively have the maximum and minimum amplitudes of fluctuations. The rainfall infiltration mostly evaporated in bare land whereas it increased the soil water content in forest-covered land.
(3) The first and the second conclusions drawn from our research may quantitatively indicate that heat and water budget analysis is a sine qua non for city planning and SALSA can be applied in such quantitative analysis and prediction.

REFERENCES

1. Brubker, K.L. and Entekhabi, D. : An analytic approach to modeling land-atmosphere interaction: Construct and equilibrium, Water Resources Research, Vol.31, No.3, pp.619-632, 1995.

2. Cary, J.W. : Soil heat transducers and water vapor flow, Soil Science of American Journal, Vol.43, pp.835-839, 1979.

3. De Vries, D.A. : Simultaneous transfer of heat and moisture in porous media, Transactions, American Geophysical Union, Vol.39, No.5, pp.909-916, 1958.

4. Entekhabi, D. and Brubker, K.L. : An analytic approach to modeling land-atmosphere interaction: Stochastic formulation, Water Resources Research, Vol.31, No.3, pp.633-643, 1995.

5. Fukuhara, T.; Pinder; G.F. and Sato, K. : An approach to fully coupled heat and moisture transfer analysis in saturated-unsaturated porous media during surface evaporation, Proc. of Japan Society for Civil Engineers (JSCE), No.423/II-14, pp.111-120, 1990.

6. Garrat, J.R. : The Atmospheric Boundary Layer, Cambridge atmospheric and space science series, Cambridge University Press, Great Britain, 1992.

7. Milly, P.C.D. : Moisture and heat transport in hysteric, inhomogeneous porous media: A matric head-based formulation and a numerical model, Water Resources Research, Vol.18, pp.489-498, 1982.

8. Milly, P.C.D. : Unsaturated flow induced by evaporation and transpiration, Unsaturated Flow in Hydrologic Modeling, Theory and Practice, H.J. Morel-Seytoux Eds., Kluwer Academic Publishers, pp.221-240, 1989.

9. Milly, P.C.D. : Effects of thermal vapor diffusion on seasonal dynamics of water in unsaturated zone, Water Resources Research, Vol.32, No.3, pp.509-518, 1996.

10. Oke, T.R. : Boundary Layer Climates, second edition, Cambridge University Press, Great Britain, 1972.

11. Pham Hong Son and Sato, K. : Heat and mass transfer between soil and atmosphere: Hanno case study, Annual Journal of Hydraulic Engineering (JSCE), Vol.43, pp.61-66, 1999.

12. Phillip, J.R. and De Vries, D.A. : Moisture movement in porous materials under temperature gradients, Transactions of the American Geophysical Union, Vol.38, pp.222-231, 1957.

13. Sang-ok, C. and Horton, R. : Soil heat and water flow with partial surface mulch, Water Resources Research, Vol.23, No.12, pp.2175-2186, 1987.

14. Siebert, J.; Sievers, U. and Zdunkowski, W. : A one-dimensional simulation of the interaction between land surface processes and the atmosphere, Boundary-Layer Meteorology, Vol.59, pp.1-34, 1992.

15. Sophocleous, M. : Analysis of water and heat flow in unsaturated-saturated porous media, Water Resources Research, Vol.15, pp.2295-1206, 1979.

16. ten Berge, H.F.M. : Heat and Water Transfer in Bare Topsoil and the Lower Atmosphere, Center for Agricultural Publishing and Documentation (Pudoc), Wageningen, the Netherlands, 1990.

17. Tennekes, H. and Lumley, J.L. : A First Course in Turbulence, The MIT Press, Cambridge, Massachusetts, 1972.

18. Tzimopoulos, C. and Sidiropoulos, E. : Coupled heat and moisture transfer in unsaturated porous bodies, Flow and Transport in Porous Media, A. Verruijt & F.B.J. Barends, Eds., A.A. Balkema Totterdam, pp.169-172, 1981.

(Received January 17, 2001 ; revised May 14, 2001)